Analytical and Bioanalytical Chemistry (2021) 413:3193–3199
https://doi.org/10.1007/s00216-021-03256-0

RESEARCH PAPER

Novel gene-encoded intermolecular FRET sensor for tracking glycosylation of CD147 in living cells

Hui Lu[1] · Lingling Zhu[1] · Wenqian Li[1] · Shuangyun Hu[2] · Yushu Ge[1] · Dan Liu[1,3]

Received: 14 December 2020 / Revised: 28 January 2021 / Accepted: 26 February 2021 / Published online: 23 March 2021

Abstract

CD147 is involved in various physiological processes and plays important roles for tumor metastasis. Glycosylation of the protein determines numerous functions of CD147. Up to now, hardly any sensor has been developed for detecting glycosylation of CD147 in live cells. There is a pressing requirement of development of a selective and continuous biosensor for cell imaging. The emergence of gene-encoded fluorescence resonance energy transfer (FRET) sensor provides a new way to develop the sensors to analysts. We designed and constructed novel gene-encoded FRET proteins sensing glycosylation of CD147 by measuring FRET ratio of two intermolecular motifs. With the decrease of CD147 glycosylation level in cells, the FRET ratio increased significantly. The specificity of the sensor targeting to CD147 was also determined by siRNA interference experiment. Finally, continuous living cell image of deglycosylation process of CD147 using the newly developed sensor has been performed successfully. The work not only provides useful tools for analyzing glycosylation of CD147 in living cells, but also implicates alternative strategy for detecting other glycosylated proteins.

Keywords CD147 · Glycosylation · FRET sensors

Introduction

CD147, also known as an extracellular matrix metalloproteinase-inducing factor or Basigin, is a type 1 transmembrane glycoprotein that belongs to the immunoglobulin superfamily [1], and is distributed on the cytoplasm and cell membrane [2]. It is involved in various physiological processes such as embryonic development, wound healing, inflammation, atherosclerosis, and arthritis [3, 4]. In addition, CD147 also promotes basement membrane degradation, matrix penetration, and cell migration during tumor metastasis by activating the matrix metalloproteinases (MMPs) [5].

Human CD147 is an N-linked glycoprotein that could be classified into the HG-CD147 (40–60 kDa) and LG-CD147 (32 kDa) forms according to different molecular weight caused by glycosylation. The molecular weight of unglycosylated core CD147 is 27 kDa [6]. Studies show that glycosylation of CD147 influences its physiological functions significantly. The deglycosylated CD147 purified from tunicamycin-treated tumor cells could not be able to stimulate the production of MMP-1 and MMP-2 [7]. Furthermore, glycosylated eukaryotic CD147 can activate MMPs more effectively than non-glycosylated prokaryotic CD147, which underscores the role of glycosylation in CD147 function [8]. Toole et al. showed that if the sugar chain of CD147 is abnormal, CD147 cannot induce the production of MMP2 normally [9]. Jia et al. found that liver cancer cell lines with stronger lymphatic metastasis ability have a higher HG-CD147/LG-CD147 ratio compared to cells lacking the ability to metastasize [10].

Therefore, monitoring the CD147 glycosylation level can indirectly reflect its biological function and tumor-related physiological characteristics. The presence of sugar chains in glycosylated proteins is mainly detected by enzymatic

Hui Lu and Lingling Zhu contributed equally to this work.

✉ Yushu Ge
geyushu@ustc.edu.cn

✉ Dan Liu
dliu919@ustc.edu.cn

[1] Hefei National Laboratory for Physical Sciences at Microscale, the CAS Key Laboratory of Innate Immunity and Chronic Disease, School of Basic Medical Sciences, Division of Life Sciences and Medicine, University of Science and Technology of China, Hefei 230027, Anhui, China

[2] Abbisko Therapeutics Co., Ltd., Shanghai 200120, China

[3] The First Affiliated Hospital of University of Science and Technology of China, Hefei 230001, Anhui, China

methods [11], lectin blotting [12], mass spectrometry [13], etc. None of these techniques can detect the glycosylation level in live cells continuously and specifically. Therefore, to further study the mechanism of CD147 glycosylation and its promotion of tumor metastasis, it is necessary to develop a probe that can specifically target the CD147 glycosylation modification level at the level of living cells. This can also fill the gap in the visual detection of glycosylation. According to the principle of fluorescence resonance energy transfer (FRET), non-radiative transfer of electron excitation from donor fluorophore to acceptor is mediated by electron dipole-dipole coupling. The transfer rate and final readout depend non-linearly on the distance between donor and acceptor [14]. We designed a FRET-based sensor for detecting glycosylation level of CD147 in live cells using CFP-S100A9 and YFP-E-selectin as the donor and acceptor. S100A9 binds to the CD147 core protein under physiological conditions specifically. Toshihiko et al. showed that S100A9 mediates inflammation and metastasis of tumor cells by interacting with the CD147 protein [15]. E-selectin interacts with the CD147 sugar chain [16]. Noritoshi et al. found that the E-selectin/CD147 could directly interact with each other during renal inflammation process [16]. Furthermore, the unglycosylated CD147 in wild-type leukocytes cannot effectively bind to E-selectin, indicating that the sugar chain structure of CD147 plays a key role for E-selectin interaction [16]. The minimum binding domain of E-selectin consists of a terminal glycan structure that contains sialic acid and fucose residues, namely tetrasaccharide sialylated-LewisX (sLeX) and sialylated-Lewis A (sLeA). Both terminal glycans are often present on the surface of various cancer cells [17]. Yang et al. showed that CD147 is one of the sialylated proteins associated with metastasis, indicating that the sialylated-LewisX structure exists at the end of the CD147 sugar chain. Thus, E-selectin is likely to interact with the sugar chain of CD147 [16, 18, 19].

In order to further study the relationship between the function of CD147 and its glycosylation. For making up for the gap in the visual detection of glycosylation, it is necessary to develop sensors that can specifically target the modification level of CD147 glycosylation. Here, we present a novel genetic-encoded FRET sensor for detecting CD147 glycosylation in live cells.

Materials and methods

Construction and transfection of plasmids

Full-length cDNAs for human CD147, S100A9, and E-selectin were synthesized by Tongyong company and cloned into the pcDNA3.1 vector using Phanta Max Super-Fidelity DNA Polymerase with mCherry, CFP, and YFP tags respectively. All plasmids were verified by DNA sequencing and the plasmid sequences are available on request. HeLa cells were transiently transfected with the different constructs using Lipofectamine 3000 (Invitrogen) according to the manufacturer's instructions. Briefly, the cells were seeded in a 6-well plate at the density of 5×10^4 cells per well, and transfected with 2.4 μg plasmid. The medium was changed 6 h after transfection.

Cell culture

The HeLa cell line was obtained from the Cell Bank of the Chinese Academy of Sciences (Shanghai, China). HeLa cells were cultured in Dulbecco's modified Eagle's medium (DMEM; BI company) supplemented with 10% (vol/vol) fetal bovine serum (FBS; BI company) and 1% (vol/vol) antibiotics (penicillin and streptomycin) at 37 °C under 5% CO_2.

Western blotting

The suitably treated HeLa cells were lysed with RIPA lysis buffer (Beyotime) for 30 min on ice, and the protein content in the lysates was determined by BCA assay (Biosharp). Equal amounts of protein per sample were denatured by boiling and separated by 12% sodium dodecyl sulfate-polyacrylamide gel electrophoresis (SDS-PAGE) and transferred to a PVDF membrane (Immobilon-P, Millipore) using transfer buffer (200 mM glycine, 25 mM Tris, 20% absolute ethanol). The membranes were blocked with 5% skimmed milk in 1× Tris-buffered saline Tween 20 (TBST; 20 mM Tris-HCl pH 8, 150 mM NaCl, 0.05% Tween 20) for 2 h at room temperature, followed by overnight incubation with anti-CD147 (Proteintech, 66443-1-lg, 1:10000), anti-GFP (Proteintech, 66002-1-lg, 1:5000), and anti-GAPDH (Proteintech, 60004-1-lg, 1:2000) primary antibodies at 4 °C. After washing thrice with TBST for 30 min each, the membranes were incubated with peroxidase-conjugated goat anti-mouse (Proteintech, 1:5000) secondary antibodies at room temperature for 2 h. The membranes were washed thrice with TBST and visualized with ECL chemiluminescence.

Co-immunoprecipitation assay

HeLa cells transfected with pcDNA3.1-YFP-E-selectin or pcDNA3.1-YFP were lysed as described above, and the crude lysates were centrifuged at 14,000*g* for 15 min at 4 °C. After removing non-specific proteins with protein G-conjugated magnetic beads (Santa Cruz) for 1 h at 4 °C, the lysates were centrifuged at 14,000×*g* for 10 min at 4 °C. The supernatants were aspirated and incubated with anti-GFP antibody (Proteintech, 50430-2-AP) for 12 h at 4 °C with constant shaking, followed by protein G magnetic beads (Santa Cruz) for 5 h at 4 °C. The beads were washed thrice with lysis buffer, and the proteins were eluted by boiling in 1× SDS loading

buffer and analyzed by immunoblotting as described. The interaction between S100A9 and CD147 was similarly evaluated.

ShRNA knock down

shCD147-pLKO.1-TRC vector was synthesized by Addgene (Hunan, China). And the shRNA sequence of human CD147 was 5′-GTACAAGATCACTGACTCT-3′ [20]. Then the shCD147-pLKO.1-TRC cloning vector system was used to produce the lentiviruses in 293 T cells. Viral supernatant fractions were collected 48 h after transfection, filtered, and centrifuged to remove cell debris. HeLa cells were transduced with the viral supernatant with 2 μg/ml polybrene, and selected 24 h after infection using 3 μg/ml puromycin. The established stable cell lines were attested western blotting analyses and used for subsequent experiments.

Fluorescence microscopy

HeLa cells were seeded at an appropriate density per well on 18 × 18-mm glass cover slips and transfected as described. The medium was replaced after 24 h with L-15 medium containing 10% (vol/vol) FBS and 1% (vol/vol) antibiotics. Stable transfectants expressing CFP-, YFP-, or mCherry-fusion were observed under a rotary disk confocal microscope (Nikon ECLIPSE Ti) at × 100 magnification, and the images were analyzed using IQ 3.0 software. The excitation wavelengths of CFP, YFP, and mCherry fluorescent protein are 445 nm, 488 nm, and 594 nm respectively.

Data analysis

FRET ratio (YFP/CFP) data were presented as mean ± SD of one representative experiment. Each experiment was repeated at least three times. Images were analyzed by ImageJ and MATLAB software. Statistical analyses were performed using GraphPad Prism 8.0 software, and unpaired two-tailed Student's *t* test was used to compare two groups. $P < 0.05$ was considered statistically significant.

Results

Structure and design of CD147 glycosylation sensor

The CD147 glycosylation sensor was constructed using CFP-S100A9 and YFP-E-selectin (Fig. 1). Simultaneous binding of S100A9 and E-selectin to the corresponding segments of CD147 altered the distance between CFP-S100A9 and YFP-PHA-L, which altered the FRET ratio. Cyan fluorescent protein (CFP) and S100A9 were connected by two flexible repeated GGSGG sequence (linkers). The yellow fluorescent protein (YFP) was connected to the lec and egf domains of E-selectin with eight GGSGG repeats. In order to ensure the detecting efficiency, we tested different binding sites on YFP and E-selectin (lec, egf, CR1, and CR2) and linkers of varying lengths (see Supplementary Information (ESM) Table S1). Finally, YFP-8 × GGSGG-lec-egf was selected for further studies. It could be speculated that the placement of YFP at the N terminal of E-selectin and a sufficient long linker were necessary for high response of the sensor.

Glycosylation sensors can respond to the decrease of CD147 glycosylation level effectively

As shown in Fig. S1 (see ESM), CD147-mCherry localized to the cell membrane and cytoplasm, CFP-S100A9 was evenly expressed in the cytoplasm and only sparsely in the nucleus, and YFP-E-selectin was uniformly expressed in both cytoplasm and nucleus. Therefore, both CFP-S100A9 and YFP-E-selectin co-localized with CD147. We tested the efficacy of the sensor by downregulating glycosylation level of CD147 with tunicamycin (TM), a broad-spectrum N-glycan inhibitor [13]. The cells were treated with varying doses (0, 0.5, 1, 2, and 3 μg/ml) of TM (Fig. 2a), and the levels of glycosylated CD147 were detected by SDS-PAGE. The proportion of HG-CD147 was obviously higher than that of LG-CD147 in the presence of 0.5 μg/ml TM. The bands corresponding to core CD147 began to appear when the TM dose was increased to 1 μg/ml. Further increasing of TM led to gradual increase in the core protein bands along with the decrease in LG-CD147. Furthermore, adding TM of concentration higher than 2 μg/ml shows cytotoxicity and results in poor growth and rounded cells. Therefore, 1 μg/ml TM was used to treat cells in the following co-transfection experiments with CFP-S100A9 and YFP-E-selectin. As shown in Fig. 2b, the FRET ratio of CFP to YFP increased by 39% in the co-transfected cells after treating with TM. Consistent with this, the cell images colored by FRET ratio values exhibited yellow and purple fluorescence before and after TM treatment respectively (Fig. 2c). The increase in FRET ratio was clearly due to the proximity between the fluorophores resulting from TM-induced decrease in CD147 glycosylation levels. The result indicated that the CFP-S100A9/YFP-E-selectin sensor was responsive to the changes in CD147 glycosylation level. To further verify that the change of FRET ratio values was not due to the expression level interference caused by adding TM, we co-transfected the cells with YFP-E-selectin/CFP and YFP/CFP-S100A9, respectively, as well as treated them with TM. As shown in Fig. S2 (see ESM), no significant change of the FRET ratio has been observed, indicating that observed FRET ratio change was dedicated by binding of S100A9 and E-selectin to the specific domains on CD147, not potential expression level relative change. Taken together, the CFP-S100A9/YFP-

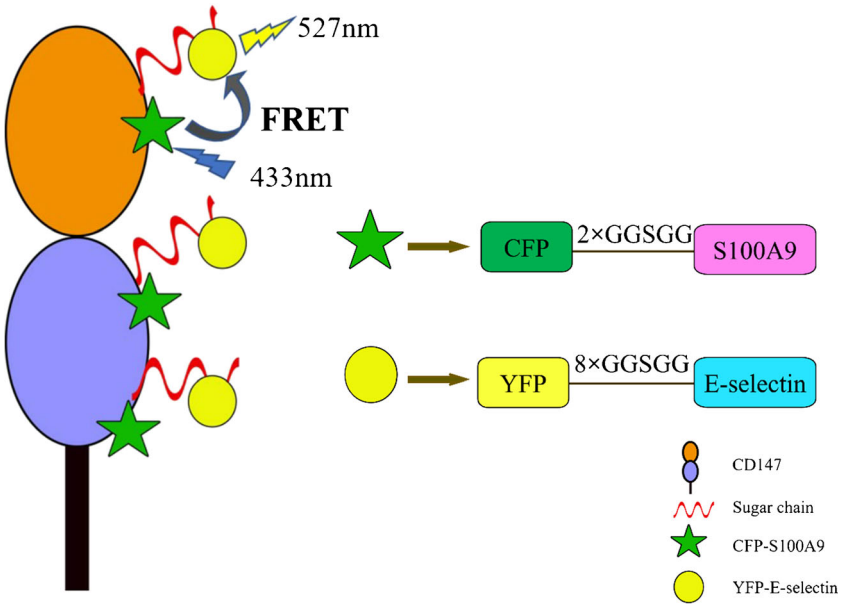

Fig. 1 Design of CD147 glycosylation sensor. The orange circle, blue circle, and black rectangle constitute the CD147 core protein structure. The red curve represents the sugar chain at the asparagine residue. The green star represents CFP-S100A9, and the yellow circle represents YFP-E-selectin. When the distance between YFP and CFP is appropriate, YFP can be excited by the emission light of CFP to produce the FRET effect. CFP and S100A9 are connected by 2 × GGSGG sequence, and YFP and E-selectin are connected by 8 × GGSGG sequence

E-selectin sensor responds to the decrease in CD147 glycosylation levels successfully.

Glycosylation sensors can respond to changes in CD147 glycosylation level specifically

Since TM is a broad-spectrum glycosylation inhibitor and does not target CD147 selectively, we knocked down CD147 using the shRNA construct in wild-type cells and observed a significant reduction in the protein levels in stable shCD147 transgenic cells (Fig. 3a). With lack of the target, the FRET ratio of the glycosylation sensor fails to change significantly after TM treatment (Fig. 3b). Due to the reduced CD147 levels, TM-induced change in the level of glycosylated CD147 was also limited, which leads to limited change in FRET ratio. Consistent with this, the FRET ratio images of CD147 knockdown cells still preform as yellow imaging even after TM treatment (Fig. 3c). Interestingly, overexpression of CD147 also did not significantly alter the FRET ratio despite an increase in the initial fluorescence (ESM Fig. S3). This is

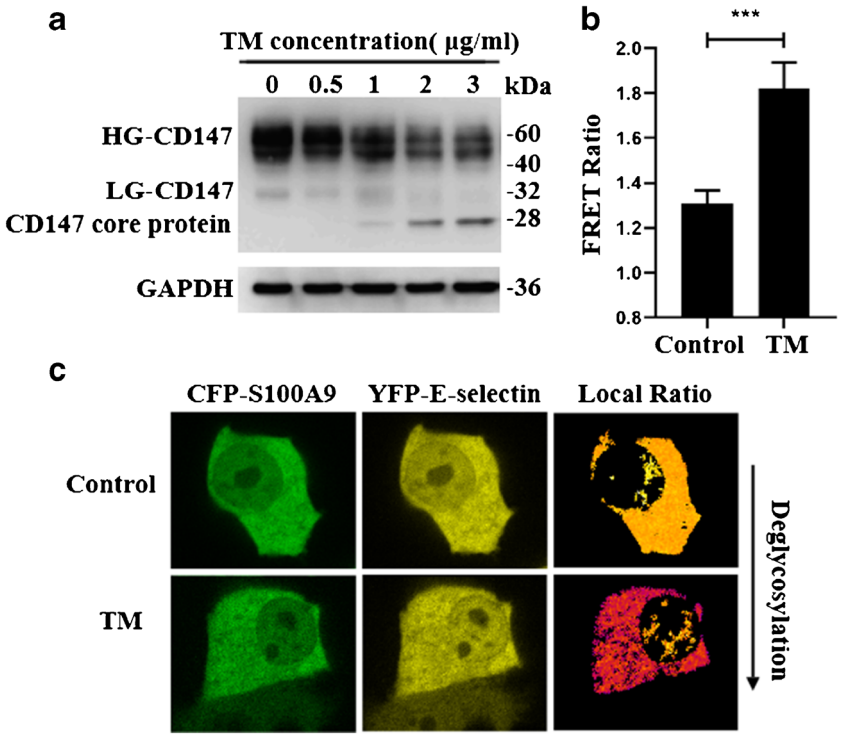

Fig. 2 TM-induced changes in CD147 glycosylation and sensor efficiency. **a** Immunoblot showing relative expression of differentially glycosylated CD147 in the presence of varying doses of TM. **b** The FRET ratio of CFP-S100A9 and YFP-E-selectin in response to TM-induced changes in CD147 glycosylation levels. **c** Representative images of co-transfected cells showing fluorescence change before and after TM treatment

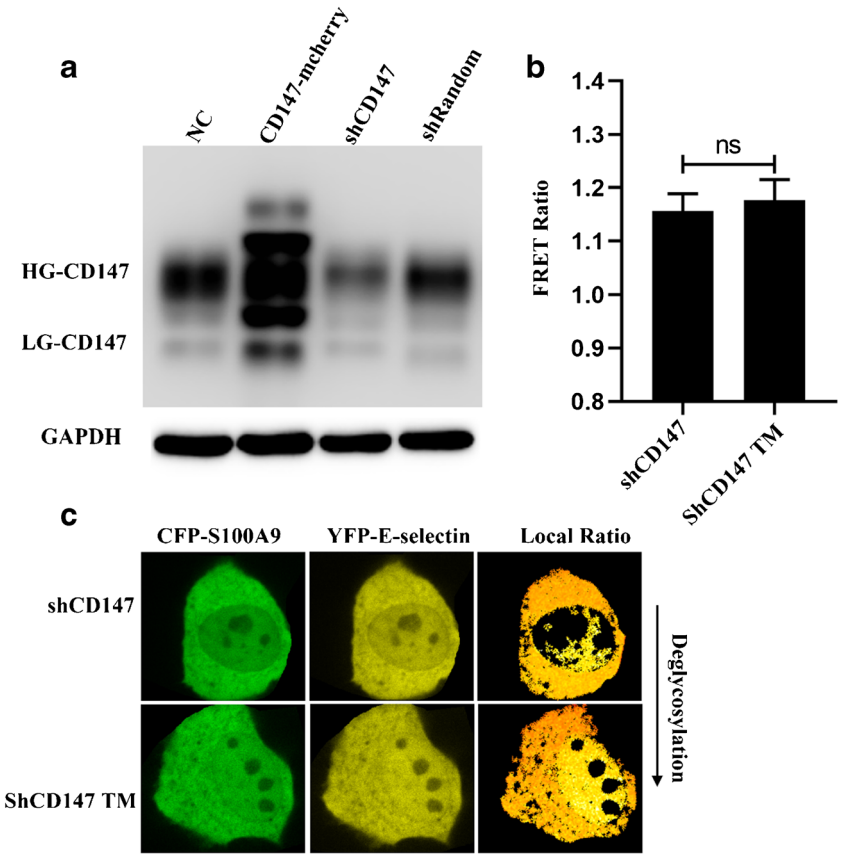

Fig. 3 Specificity of the CFP-S100A9/YFP-E-selectin sensor to CD147 glycosylation. **a** Immunoblot showing CD147 overexpression and knockdown (NC is the negative control, and shRandom is the scramble shRNA control). **b** The FRET ratio of CFP-S100A9 and YFP-E-selectin in the TM-treated shCD147 cells. **c** Representative images of shCD147 cells showing fluorescence change before and after TM treatment

possibly due to the fact that overexpression of CD147 did not affect the extent of its glycosylation after TM treatment. Taken together, the CFP-S100A9/YFP-E-selectin glycosylation sensor could respond to CD147 specifically.

Glycosylation sensors directly interact with CD147

The specific interaction between CD147 and the CFP-S100A9/YFP-E-selectin sensor was evaluated by the co-immunoprecipitation assay. The cells were transfected with the CFP empty plasmid or CFP-S100A9 and treated with TM. As shown in Fig. 4a, the cells expressed CFP or CFP-S100A9, and the levels of glycosylated CD147 were reduced after TM treatment. In addition, the anti-CFP antibody successfully pulled down CD147 along with CFP-S100A9 regardless of TM, whereas CFP alone did not co-precipitate with CD147 protein. Furthermore, HG-CD147 showed the strongest co-precipitation with CFP-S100A9, whereas LG-CD147 interacted weakly with the sensor protein. Similar co-IP experiment was performed in cells transfected with YFP or YFP-E-selectin. As shown in Fig. 4b, the anti-GFP antibody pulled down CD147 with YFP-E-selectin and not YFP. The major fraction of the co-precipitated CD147 was about 40 kDa high glycosylated form, followed by the 60 kDa and the low glycosylated form of molecular weight about 30 kDa. Finally, the CD147 co-precipitated by YFP-E-selectin and CFP-S100A9 had the same molecular weight, indicating that both sensors have consistent efficiency. Therefore, CFP-S100A9 and YFP-E-selectin directly interact with CD147 domains in living cells. We also performed a quantitative analysis of the co-IP results in Fig. 4. The results are shown in Fig. S5 of the ESM.

The sensors can dynamically track the reduction of CD147 glycosylation level in live cells

To determine whether the CFP-S100A9/YFP-E-selectin sensor can detect the changes in CD147 glycosylation levels in real time, the cells were treated with 2 μg/ml TM continuously for 12 h. As shown in Fig. 5c, CD147 glycosylation levels did not decrease significantly in the first 2 h, and LG-CD147 and core CD147 appeared thereafter. The amount of core CD147 increased in a time-dependent manner, whereas LG-CD147 disappeared after 8 h. The overall CD147 glycosylation levels decreased within the first 6 h. The reason why the TM concentration is 2 μg/ml instead of 1 μg/ml is that after 1 μg/ml TM treats the cells, the glycosylation level of CD147 is not significantly reduced within 6 h (ESM Fig. S4). When the cells were treated with 2 μg/ml TM, the glycosylation level of CD147 decreased significantly within 6 h. The FRET ratio of the sensor increased sharply in the first 3 h, and steadily plateaued with the time-dependent decline in CD147 glycosylation levels (Fig. 5b). As

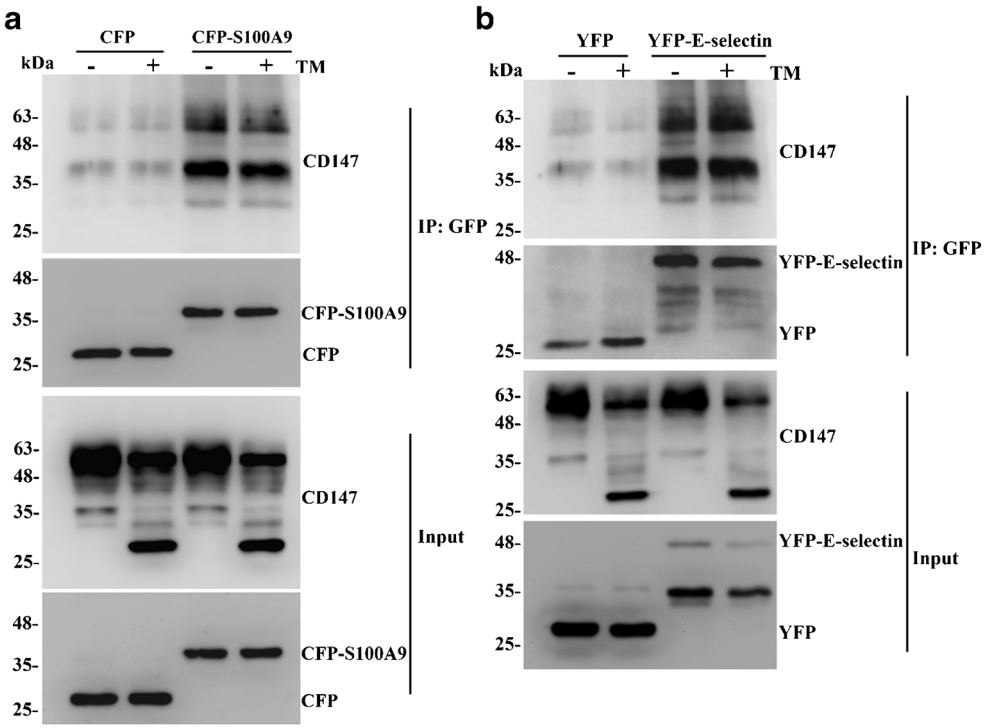

Fig. 4 Co-IP showing intracellular interaction of CFP-S100A9 and YFP-E-selectin with CD147. **a** Immunoblots showing co-precipitation of CD147 with CFP and CFP-S100A9 by anti-CD147 (image 1) and anti-GFP (image 2) antibodies, expression of CD147 (image 3), and expression of CFP and CFP-S100A9 (image 4). **b** Immunoblots showing co-precipitation of CD147 with YFP and YFP-E-selectin by anti-CD47 (image 1) and anti-GFP (image 2) antibodies, expression of CD147 (image 3), and expression of YFP and YFP-E-selectin (image 4)

expected, the FRET ratio was unaltered in the control cells, and the curve was relatively flat. Since the cells under the TM culture condition were continuously exposed to laser irradiation, most of them started to round or even died after 6 h. Therefore, only the data of the first 5 h were used for statistical analysis. Consistent with the change in FRET ratio, the FRET ratio imaging of the cells steadily darkened from yellow to purple with prolonged TM treatment (Fig. 5a). Taken together, the CFP-S100A9/YFP-E-selectin sensor can detect the dynamic changes in CD147 glycosylation that can be read both visually and in terms of FRET ratios. Then, we performed a quantitative analysis of CD147 on the results of Fig. 5c, and quantified the amount of HG-CD147 decreased with the increase of TM treatment time (ESM Fig. S6a). And we analyzed the relationship between the FRET ratio of the sensor and the reduction in CD147 glycosylation (ESM Fig. S6b) at the corresponding time (0, 1, 2, 4 h) of the TM treatment. From Fig. S6b, it can be seen that in the first 2 h, the FRET ratio will increase by 0.2 for every 5% decrease in

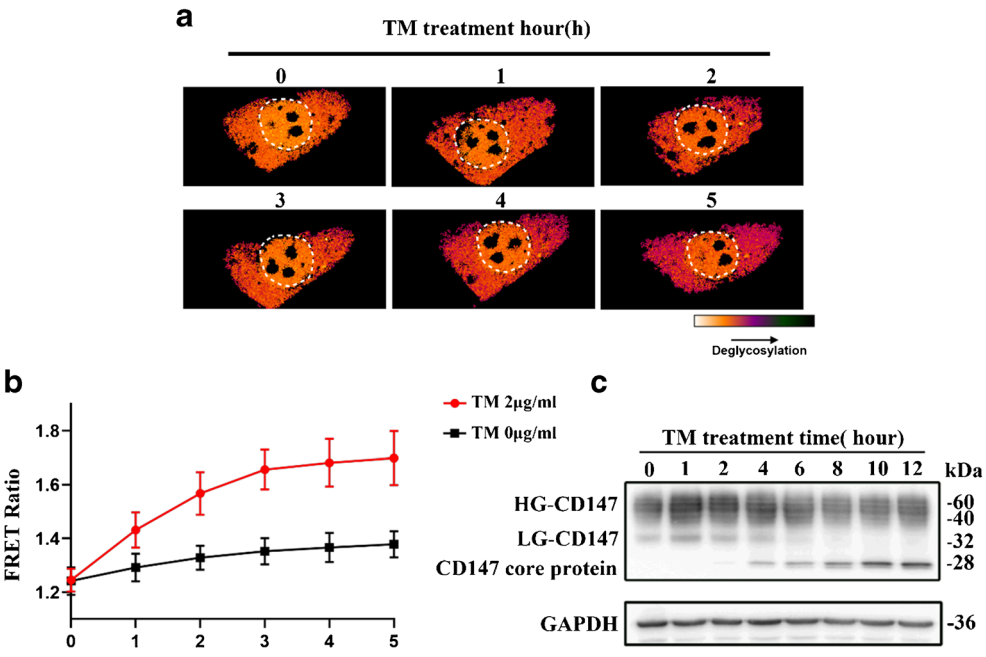

Fig. 5 CFP-S100A9/YFP-E-selectin sensor detects dynamic changes in CD147 glycosylation in the presence of TM. **a** Representative images of cells showing changes in fluorescence in response to continuous TM exposure. The white dotted line indicates the nucleus. **b** FRET ratio in cells treated with 0 or 2 μg/ml TM for 12 h. The red and black discontinuous lines indicate 2 μg/ml and 0 μg/ml TM respectively. **c** Immunoblot showing changes in CD147 glycosylation levels during the 12-h TM treatment

CD147 glycosylation level. But as the TM processing time increases, the rate of increase of the FRET ratio value becomes slower. This may be due to the annihilation of sensor fluorescence as the laser irradiation time increases during microscope shooting.

Conclusion

In general, the novel developed pair of sensors could specifically and dynamically detect the glycosylation level of CD147 in living cells. Direct interaction between CD147 and sensor has been confirmed. Significant FRET ratio changes have been observed with downregulating glycosylation level of CD147 using TM inhibitor. The specificity of the sensor was also confirmed through interference expression level of CD147. Finally, the real-time imaging for continuous reduction of CD147 glycosylation has been established in live cells successfully. The sensor is quite suitable for detecting immature glycosylation CD147 in the cytoplasm, which makes it possible to explore the dynamic changes and potential cellular process of intracellular CD147 glycosylation. In addition, considering the design principle based on the specific binding domain for targeting protein and modified sugar chain, it could be speculated that similar sensors aiming to detect other protein glycosylation might also be able to develop a simple replacement of S100A9. Furthermore, detecting other types of glycosylation is also possible by using other candidates instead of E-selection.

Supplementary Information The online version contains supplementary material available at https://doi.org/10.1007/s00216-021-03256-0.

Funding This research was funded by Major Research Plan of the National Natural Science Foundation of China(2016YFA0101200), National Natural Science Foundation of China (Projects 21778050, 91749125), Youth Fund of National Natural Science Foundation of China (81701232), New Medical Science Joint Fund of USTC (WK2070000123), and Training Program of the Major Foundation of USTC (WK3520000007).

Declarations

Conflict of interest The authors declare no conflict of interest.

References

1. Zhu X, Wang S, Shao M, Yan J, Liu F. The origin and evolution of Basigin (BSG) gene: a comparative genomic and phylogenetic analysis. Dev Comp Immunol. 2017;72:79–88.
2. Lu M, Wu J, Hao ZW, Shang YK, Xu J, Nan G, et al. Basolateral CD147 induces hepatocyte polarity loss by E-cadherin ubiquitination and degradation in hepatocellular carcinoma progress. Hepatology. 2018;68(1):317–32.
3. Agrawal SM, Yong VW. The many faces of EMMPRIN - roles in neuroinflammation. Biochim Biophys Acta. 2011;1812(2):213–9.
4. Schmidt R, Bultmann A, Fischel S, Gillitzer A, Cullen P, Walch A, et al. Extracellular matrix metalloproteinase inducer (CD147) is a novel receptor on platelets, activates platelets, and augments nuclear factor kappaB-dependent inflammation in monocytes. Circ Res. 2008;102(3):302–9.
5. Huang P, Chang S, Jiang X, Su J, Dong C, Liu X, et al. RNA interference targeting CD147 inhibits the proliferation, invasiveness, and metastatic activity of thyroid carcinoma cells by downregulating glycolysis. Int J Clin Exp Pathol. 2015;8(1):309–18.
6. Bai Y, Huang W, Ma LT, Jiang JL, Chen ZN. Importance of N-glycosylation on CD147 for its biological functions. Int J Mol Sci. 2014;15(4):6356–77.
7. Sun J, Hemler ME. Regulation of MMP-1 and MMP-2 production through CD147/extracellular matrix metalloproteinase inducer interactions. Cancer Res. 2001;61(5):2276–81.
8. Huang W, Luo WJ, Zhu P, Tang J, Yu XL, Cui HY, et al. Modulation of CD147-induced matrix metalloproteinase activity: role of CD147 N-glycosylation. Biochem J. 2013;449(2):437–48.
9. Toole BP. Emmprin (CD147), a cell surface regulator of matrix metalloproteinase production and function. Curr Top Dev Biol. 2003;54:371–89.
10. Jia L, Zhou H, Wang S, Cao J, Wei W, Zhang J. Deglycosylation of CD147 down-regulates matrix metalloproteinase-11 expression and the adhesive capability of murine hepatocarcinoma cell HcaF in vitro. IUBMB Life. 2006;58(4):209–16.
11. Hirabayashi J, Kasai K. Separation technologies for glycomics. J Chromatogr B Analyt Technol Biomed Life Sci. 2002;771(1–2):67–87.
12. Dai Z, Zhou J, Qiu SJ, Liu YK, Fan J. Lectin-based glycoproteomics to explore and analyze hepatocellular carcinoma-related glycoprotein markers. Electrophoresis. 2009;30(17):2957–66.
13. Sugyo A, Tsuji AB, Sudo H, Nagatsu K, Koizumi M, Ukai Y, et al. Evaluation of (89)Zr-labeled human anti-CD147 monoclonal antibody as a positron emission tomography probe in a mouse model of pancreatic cancer. PLoS One. 2013;8(4):e61230.
14. Prevo B, Peterman EJ. Forster resonance energy transfer and kinesin motor proteins. Chem Soc Rev. 2014;43(4):1144–55.
15. Hibino T, Sakaguchi M, Miyamoto S, Yamamoto M, Motoyama A, Hosoi J, et al. S100A9 is a novel ligand of EMMPRIN that promotes melanoma metastasis. Cancer Res. 2013;73(1):172–83.
16. Kato N, Yuzawa Y, Kosugi T, Hobo A, Sato W, Miwa Y, et al. The E-selectin ligand basigin/CD147 is responsible for neutrophil recruitment in renal ischemia/reperfusion. J Am Soc Nephrol. 2009;20(7):1565–76.
17. Carrascal MA, Silva M, Ferreira JA, Azevedo R, Ferreira D, Silva AMN, et al. A functional glycoproteomics approach identifies CD13 as a novel E-selectin ligand in breast cancer. Biochim Biophys Acta Gen Subj. 2018;1862(9):2069–80.
18. Miyauchi T, Kanekura T, Yamaoka A, Ozawa M, Miyazawa S, Muramatsu T. Basigin, a new, broadly distributed member of the immunoglobulin superfamily, has strong homology with both the immunoglobulin V domain and the beta-chain of major histocompatibility complex class II antigen. J Biochem. 1990;107(2):316–23.
19. Yang L, Nyalwidhe JO, Guo S, Drake RR, Semmes OJ. Targeted identification of metastasis-associated cell-surface sialoglycoproteins in prostate cancer. Mol Cell Proteomics. 2011;10(6):M110 007294.
20. Li Y, Wu J, Song F, Tang J, Wang SJ, Yu XL, et al. Extracellular membrane-proximal domain of HAb18G/CD147 binds to metal ion-dependent adhesion site (MIDAS) motif of integrin beta1 to modulate malignant properties of hepatoma cells. J Biol Chem. 2012;287(7):4759–72.